Chapter 4

Simple Chaotic Models

This chapter presents a short study of simple autonomous and non-autonomous systems exhibiting strange chaotic attractors. In particular, the Lorenz and Rössler equations are discussed and the geometrical properties of the chaotic attractors governed by these equations are described. Other examples of autonomous chaotic systems include modified generators with inertial nonlinearity, Chua circuit, systems with quadratic nonlinearities, labyrynth chaos, jerk equations, two-scroll and three-scroll attractors, and Rikitake chaotic attractor.

Examples of simple non-autonomous systems generating chaos include forced van der Pol equation, Rayleigh equation, Duffing oscillator and single-well oscillator, and externally and parametrically excited oscillators.

The background given in this chapter is useful while exploring the next chapters since many of the presented and discussed chaotic attractors can also be found in the systems with infinite dimension.

4.1 Introduction

Nowadays, it is well known that numerous dynamical systems modelling phenomena met in our universe are essentially nonlinear and coupled, and cannot be presented and explained by traditional methods of mathematical analysis. It is impossible to obtain the algebraic description for solutions to the mentioned problems in closed forms, even though infinite series as well as special functions are applied. However, desirable success can be achieved with the help of numerical methods.

In many cases met in practice, the so-called transitional processes are characterized by non-stationary and nonlinear phenomena, including occurrence of large displacements of a studied system and a complex and rich mechanism of the interaction between coupled subsystems, energy pumping and dissipation. They include, for instance, problems of fluid dynamics, such as the trans-sound phenomena associated with the moving body and its interaction with the flow, and other. All of the so far described phenomena may exhibit turbulent behavior. This is why solutions to the so far mentioned problems require computers with very large memories, and with the possibility of realizing a few billions of operations per second.

The following three directions of research are associated with the qualitative analysis of nonlinear dynamical systems:

(i) Rigorous mathematical proofs and analyses of properties of hyperbolic and parabolic systems.
(ii) Construction of mathematical models of dynamics aimed at purely scientific investigations, and their qualitative analysis.
(iii) Construction and investigation of simple archetypical models exhibiting fundamental properties of chaotic systems.

The last direction of investigation attracted a lot of interest by numerous researchers, what yielded the fundamental results in the field of deterministic chaos.

4.2 Autonomous Systems

4.2.1 *Lorenz mathematical model (LMM)*

In what follows, we give a remarkable example demonstrating chaotic dynamics. In 1959, E. Lorenz began his numerical investigation of some meteorological problems including modeling and numerical simulations of convective flows in the atmosphere. The LMM has been published in 1963, i.e. before the definition of a strange attractor [Lorenz (1963)]. Lorenz aimed at a weather forecast for a longer period. Then, about thirty years later he came back to his accidently discovered sensitive dependence on initial conditions of the derived

Fig. 4.1 The Lorenz set (a photo from [www.giport.ru]).

differential equations describing atmospheric convection at the Massachusetts Institute of Technology (MIT) (see [Lorenz (1991, 1993)]). The Lorenz strange attractor is shown in Fig. 4.1.

Let us consider a fluid layer of constant thickness H, subjected to action of the temperature gradient ΔT. If all motions are parallel to the plane $(x-z)$ and they are homogenous in direction of y, then the governing equations take the following form

$$\frac{\delta}{\delta t}(\nabla^2\psi) = \frac{\delta\psi}{\delta z}\frac{\delta}{\delta x}(\nabla^2\psi) - \frac{\delta\Psi}{\delta x}\frac{\delta}{\delta z}(\nabla^2\psi + \nu\nabla^2(\nabla^2\psi)) + g\alpha\frac{\delta\theta}{\delta x},$$
$$\frac{\delta\theta}{\delta t} = \frac{\delta\theta}{\delta z}\frac{\delta\psi}{\delta x} - \frac{\delta\theta}{\delta x}\frac{\delta\psi}{\delta z} + k\nabla^2\theta + \frac{\Delta T}{H}\frac{\delta\psi}{\delta x}, \tag{4.1}$$

where ψ is the function of the 2D flow, i.e. the velocity $(u = (u, w))$ is defined by the following formulas

$$u = \frac{\delta\psi}{\delta z}, \quad W = -\frac{\delta\psi}{\delta x}, \tag{4.2}$$

where θ is the temperature field characterizing deviation from the equilibrium state; g is the Earth acceleration, α is the coefficient of the temperature extension; ν is the kinematic viscosity, k is the heat transfer coefficient.

A solution to this problem is known since Rayleigh, and it reads

$$\psi = \psi_0 \sin\left(\frac{\pi\alpha x}{H}\right)\sin\left(\frac{\pi z}{H}\right), \quad \theta = \theta_0 \cos\left(\frac{\pi\alpha x}{H}\right)\sin\left(\frac{\pi z}{H}\right). \tag{4.3}$$

The given solution starts to increase if the Rayleigh number $R_\alpha = \frac{g\alpha H^3\Delta T}{\gamma k}$ exceeds the following critical value

$$R_\alpha^+ = \frac{\pi^4(1-\alpha^2)^3}{\alpha^2}, \tag{4.4}$$

$$\min R_\alpha^+ = \frac{27\pi}{4} = 657.511 \quad \text{for } \alpha^2 = \frac{1}{2}. \tag{4.5}$$

One may solve system (4.1) in higher order approximations, when instead of the simple Rayleigh approximation (4.3), the following one is applied

$$\psi(x,\, z,\, t) = \sum_{m=1}^{\infty}\sum_{n=1}^{\infty}\psi_{mn}(t)\sin\left(\frac{m\pi\alpha x}{H}\right)\sin\left(\frac{n\pi x}{H}\right),$$
$$\theta(x,\, z,\, t) = \sum_{m=1}^{\infty}\sum_{n=1}^{\infty}\theta_{mn}(t)\cos\left(\frac{m\pi\alpha x}{H}\right)\sin\left(\frac{n\pi x}{H}\right). \tag{4.6}$$

In this case, periodic boundary conditions on both directions are formulated. Substituting (4.6) into (4.1), we get an infinite number of ordinary differential equations (ODEs).

Lorenz [Lorenz (1963)] considered the following strong truncation of the problem: $\psi_{11} = X$, $\theta_{11} = Y$ and $\theta_{02} = Z$. In this case, with the help of scaling transformations, the input system of equations has been reduced to three ODEs of the form:

$$\dot{x} = \sigma(y-z), \quad \dot{y} = -xz + rx - y, \quad \dot{z} = xy - bz, \tag{4.7}$$

where $\sigma = \nu/k$ is the Prandtl number, $r = R_\alpha/R_a^+$ is the Rayleigh normalized number, $b = 4(1+a^2)$ is the geometric factor (time variable is rescaled to the form $\tau = \pi^2(1+a^2)kt/H^2$). Equations (4.7) are known as Lorenz equations. We have the following variables: x is the convection intensity, y is the temperature difference between input and output flows, z is the deviation of the vertical temperature profile with respect to the linear one.

In what follows, we report a few properties of equations (4.7).

1. *Divergence*

$$D = \frac{\partial \dot{x}}{\partial x} + \frac{\partial \dot{y}}{\partial y} + \frac{\partial \dot{z}}{\partial z} = -(b+\sigma+1) \tag{4.8}$$

is negative, since $b > 0$, $\sigma > 0$. Let us denote the volume element of the phase space by $\Gamma(t)$, and hence a flow compression can be presented in the following form

$$\Gamma(t) = \Gamma(0)e^{-(b+\sigma+1)t}. \tag{4.9}$$

It is observed that all trajectories are bounded by a certain limiting manifold.

2. *Critical points*

Condition $x = \dot{y} = \dot{z} = 0$ is satisfied by the following points:

(a) $x = y = z = 0$ — pure heat transfer without convection;
(b) $X = Y = \pm\sqrt{b(r-1)}$, $Z = (r-1)$ — stationary convection, which is possible for $r > 1$.

3. *Stability*

We recast the linearized equations associated with (4.7) to the following matrix form

$$\frac{d}{dt}\begin{bmatrix}\delta X\\ \delta Y\\ \delta Z\end{bmatrix} = \begin{bmatrix}-\sigma & \sigma & 0\\ (r-z) & -1 & -x\\ y & x & -b\end{bmatrix}\begin{bmatrix}\delta X\\ \delta Y\\ \delta Z\end{bmatrix}. \tag{4.10}$$

Linear ODEs (4.10) allow to get some conclusions regarding stability of critical points:

(a) Point $(X,Y,Z) = (0,0,0)$ is stable for $r < 1$, i.e. all eigenvalues have negative real part; for $r > 1$, a real part of one of the eigenvalues becomes positive, i.e. the critical point becomes unstable and hence the infinite small perturbation may imply convection. Note that the stability of a critical point depends only on the Rayleigh number.
(b) Point $(X,Y,Z) = (\pm\sqrt{b(r-1)}; \pm\sqrt{b(r-1)}; r-1)$ for $r > 1$ exhibits eigenvalues consisting of one real negative root and a pair of complex conjugated roots. This pair of critical points loses its stability for

$$r = \frac{\sigma(\sigma+b+1)}{\sigma-b-1}. \tag{4.11}$$

If $r > 0$, the mentioned conditions are satisfied only in the case if $\sigma > (b+1)$.

Remark 1

It occurs that the stability of the studied critical points does not depend only on the Rayleigh number. Lorenz [Lorenz (1963)] chose the following parameters: $b = 8/3$, $\sigma = 10$. They yielded stability loss of the convective state for $r = 470/19 \approx 24.74\ldots$, $D = -13.67$. Let us divide $\{r\}$ into four intervals: (1) $0 > r > 1$, (2) $1 < r < 24.74$, (3) $r \cong 24.74$, (4) $r > 24.74$, and let us analyze a solution of Lorenz equations.

1. $r \in (0;1)$. All trajectories associated with arbitrarily chosen initial conditions move along a spiral into the coordinates origin, i.e. we have a globally attractive stationary solution.
2. $r \in (1;24.74)$. Origin loses its stability via bifurcation and is transformed into a pair of locally attracting stationary solutions: $c_1(\sqrt{b(r-1)}, \sqrt{b(r-1)}, r-1)$, $c_2(-\sqrt{b(r-1)}, -\sqrt{b(r-1)}, r-1)$. All trajectories tend either to point c_1 or c_2, possibly besides a set of trajectories of zero measure remaining in the origin neighborhood.
3. $r \approx 24.74$. We deal with a critical value, for which c_1 and c_2 lose their stability, but c_1 and c_2 do not tend to the limit cycles, since for large r an inversed bifurcation takes place.

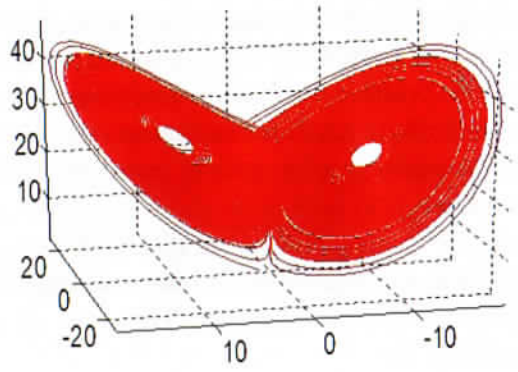

Fig. 4.2 Solution to Lorenz equations for $r = 28$, $\sigma = 10$, $b = 8/3$, $z = 27$.

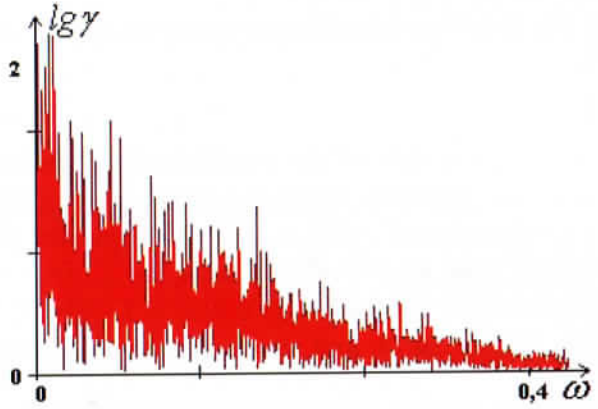

Fig. 4.3 Power spectrum of the Lorenz equations.

4. $r > 24.74$. The motion is of an essential disorder. It evolves in a spiral manner in the neighborhood of one of the fixed points (c_1 and c_2) within a certain time interval and then jumps into the neighborhood of the second fixed point in an unpredictible manner, and so on. This implies occurence of stretching and folding and creation of a complex manifold called a *strange chaotic attractor*. Typical trajectories of this attractor are reported in Fig. 4.2, whereas the associated power spectrum is shown in Fig. 4.3.

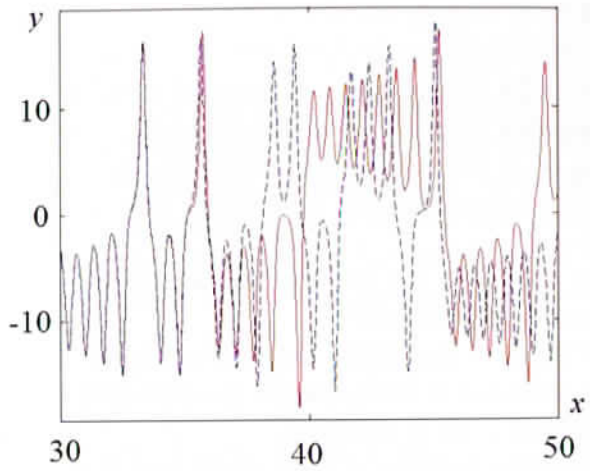

Fig. 4.4 Time history of the Lorenz equations.

Lorenz carried out long-term computations and stopped his numerical experiment. He observed a peculiar numerical behavior. Assuming that the computations will be repeated with exactly the same initial conditions, the numerical results should also be repeated. Lorenz slightly changed initial conditions, decreasing a number of less meaningful digits. Errors introduced by those changes were small. In the beginning, the obtained results coincided with the previous ones. However, the increase in the computational time yielded a new solution completely different from the previous one (Fig. 4.4). Lorenz repeated the computations many times to be sure of the obtained results. However, what has been later recognized, he experienced the high solution sensitivity to the introduced initial conditions, i.e. the fundamental property of chaotic dynamics.

The obtained dependence is referred to as a butterfly effect, which has been illustrated and discussed in his work published in 1972 with the provoking title "Does the flap of a butterfly's wings in Brazil set off a tornado in Texas?" [Lorenz (1972)]. It means that the long-term weather forecast may fail due to the sensitivity of the initial conditions (small changes may result in qualitatively different response).

Remark 2

1. For $r \approx 24.74$, the dynamics becomes chaotic, but a sequence of the associated events implies chaos does not include any periodic regimes, i.e. it does not coincide with the Ruelle–Takens scenario initiating the occurence of a turbulent flow [Ruelle and Takens (1971)].
2. For $r = 145-148$, the strange chaotic attractor is transformed into a periodic limit cycle.
3. Further increase in r forces the limit cycle to vanish, and again strange attractor is born, but for $r = 210-234$ the occurence of another limit cycle is observed.
4. While moving between a limit cycle and a strange attractor, new phenomena have been observed referred as intermittency of various types.
5. Since the studied Lorenz system is truncated, another challenging research direction concerns the increase in the number of modes in equations (4.6) to be taken into account during numerical simulations.

Remark 3

1. One of the main disadvantages of the Lorenz analysis relies on the rigorously introduced truncation of modes. Therefore, it is of interest to know what happens when the number of modes increases. The increase in the number of terms in (4.6) by one implies a series of different regimes. Though it was possible to find a strange chaotic attractor, the most sensitive parameter has been associated with a number of modes. This means that truncation of PDEs by keeping only a few modes cannot guarantee a real system behaviour.
2. In spite of the criticism introduced so far, simple models such as the Lorenz model are of interest since they may exhibit very rich nonlinear dynamics.
3. An important role is played also by the investigation of convergence of the solution series (4.1).

4. Another challenging direction of investigations of PDEs is associated with the proof of existence of attractors of finite dimensions.

Investigation of the Lorenz equations opened a challenging approach aimed at finding an even simpler set of ODEs exhibiting chaotic strange attractors. Namely, it has been observed that rescaling the Lorenz Equations (4.7) in the following way: $(x, y, z) \to (\sigma x, \sigma y, \sigma z + r)$, $t \to t/\sigma$, and taking into account $r, \sigma \to \infty$ while $r^* = br/\sigma^2$ remains finite, the so-called *diffusionless Lorenz systems* have been obtained

$$\dot{x} = y - x, \quad \dot{y} = -xz, \quad \dot{z} = xy - r^*, \tag{4.12}$$

where for wide range of only one parameter r^* a strange chaotic attractor has been detected (for instance, for $r^* = 1$ the largest Lyapunov exponent $\lambda_{\max} = 0.21$).

4.2.2 *Rössler mathematical model (RMM)*

In 1976, Rössler [Rössler (1976)] proposed the model governing a chemical reaction of the following form

$$\dot{x} = -y - z, \quad \dot{y} = x + ay, \quad \dot{z} = b - cz + xz, \tag{4.13}$$

where a, b, c are the system parameters. Lorenz in book [Lorenz (1993)] has pointed out that O. Rössler has discovered a simpler system of differential equations with chaotic solutions. The system (4.13) is recast in the following way: first equation is differentiated with respect to time, and after removing the second equation we get:

$$\ddot{x} - a\dot{x} + (1 + z)x = (a + c)z - b, \qquad \dot{z} = b - cz + xz. \tag{4.14}$$

In this case, the Rössler system can be interpreted as an oscillator with a parametric and external excitation, and their input depends on the value of the amplitude of oscillations. Increase in the parameter c yields a series of period doubling bifurcations, and then a strange chaotic attractor appears (Fig. 4.5). After achieving a critical point, a series of bifurcations matching stripes of a chaotic attractor

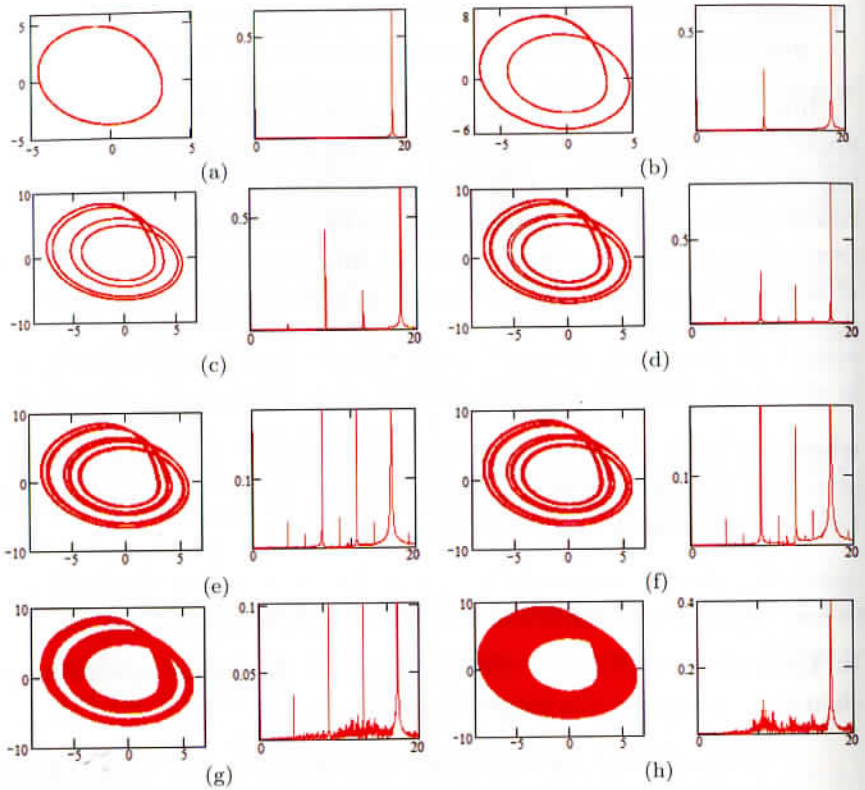

Fig. 4.5 (a) Trajectories of the Rössler equations projected into the (x, y) plane and the corresponding power spectra $a = b = 0.1$, $c = 2.6$, (b) $c = 3.5$, (c) $c = 4.1$, (d) $c = 4.18$, (e) $c = 4.21$, (f) $c = 4.23$, (g) $c = 4.3$, (h) $c = 4.6$.

appeared. The Rössler system allows for an approximation of a 3D flow into one-dimensional map [Lichtenberg and Lieberman (1984)], which is defined by the strong contraction of the phase volume into one of the eigenvectors.

Apparently, Rössler detected a simpler system exhibiting chaotic dynamics governed by the following equations [Rössler (1979)]:

$$\dot{x} = -y - z, \quad \dot{y} = x, \quad \dot{z} = a(y - y^2) - bz. \tag{4.15}$$

The Rössler prototype-4 type (4.15) displays strange chaotic attractors for $a = b = 0.5$ (in this case, $\lambda_{\max} = 0.094$).

4.2.3 *Modified generator with inertial nonlinearity (MGIN)*

The MGIN is described by the following equation [Anishchenko *et al.* (1999)] (similar to these have already been discussed in the first and second sections of this chapter):

$$\dot{x} = mx + y - xz, \quad \dot{y} = -x, \quad \dot{z} = -gz + z\Phi(x), \tag{4.16}$$

where $\Phi(x) = x^2$ (for $x \geq 0$) and $\Phi(x) = 0$ (for $x < 0$), m, g are the system parameters, and m is proportional to a difference between the input and output energies, g is the relative relaxation time of a *thermistor*. The given model is based on the classical schemes of generators, and in asymptotic cases it describes the Van der Pol generator. In a classical generator with an internal nonlinearity [Teodorchik (1964)], the self-oscillations are guaranteed by introducing a thermo-resistor into the oscillation contour, whose properties depend on the electrical loop current. Model of the generator with the inertial nonlinearity illustrates various mechanisms of occurrence of the deterministic chaos in the system with a homoclinic trajectory of the saddle-focus separatrix type. Figure 4.6 presents (a) phase portrait, (b) time history, and (c) power spectrum characterizing the period doubling scenario.

It has been verified experimentally that in all dynamical systems where chaos occurs through the period doubling bifurcations, a chaotic attractor has a fractal dimension $2 < d < 3$, and its cross-section has a horseshoe shape.

4.2.4 *Chua circuit*

Mathematical model of the Chua generator [Chua (1992); Chua *et al.* (1982, 1986)] is more complex than described in Section 4.2.2, since we have three equilibria, a symmetry and more complex types of the trajectories. Equations governing system dynamics follow

$$\dot{x} = \alpha[y - h(x)], \quad \dot{y} = x - y + z, \quad \dot{z} = -\beta y - \gamma z, \tag{4.17}$$

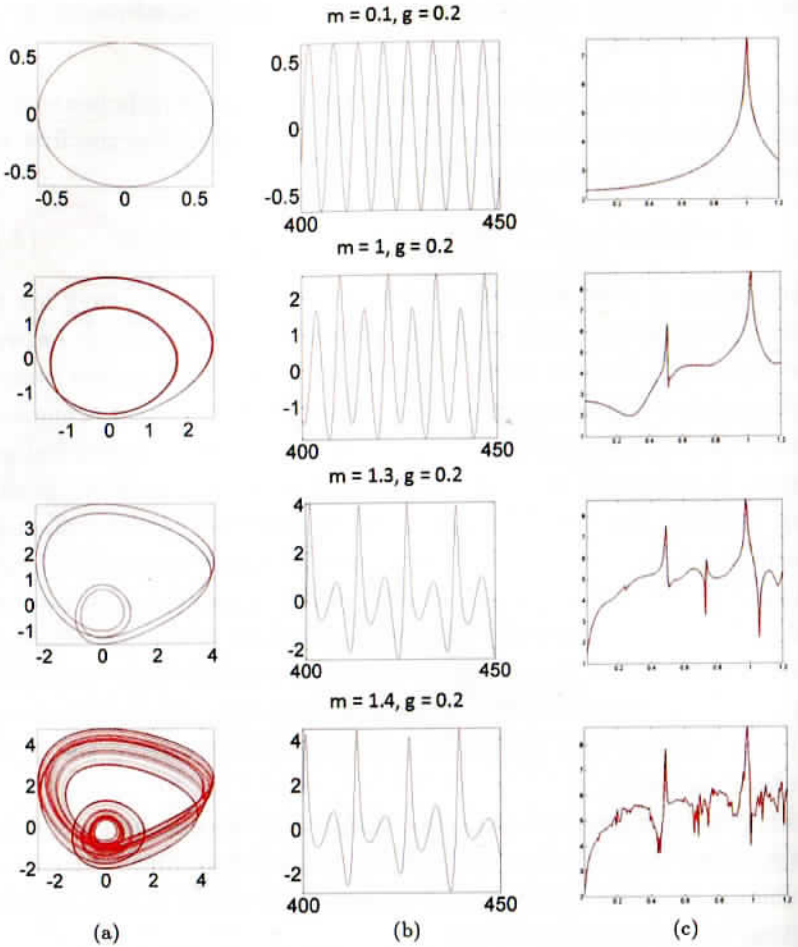

Fig. 4.6 (a) Series of period doubling bifurcations: phase portrait, (b) time history, (c) power spectrum.

where: $h(x) = bx + 0.5(a-b)(|x+1| - |x-1|)$, and a, b, α, β are the non-dimensional system coefficients. They can be recast to the following form of equations

$$\dddot{z} + \ddot{z} + \beta z = \beta x, \quad \dot{x} = -\frac{\alpha}{\beta}\dot{z} - \alpha h(x). \tag{4.18}$$

In the system (4.18), owing to the symmetry, a doubled loop of the saddle-focus separatrix is constructed which is responsible for the

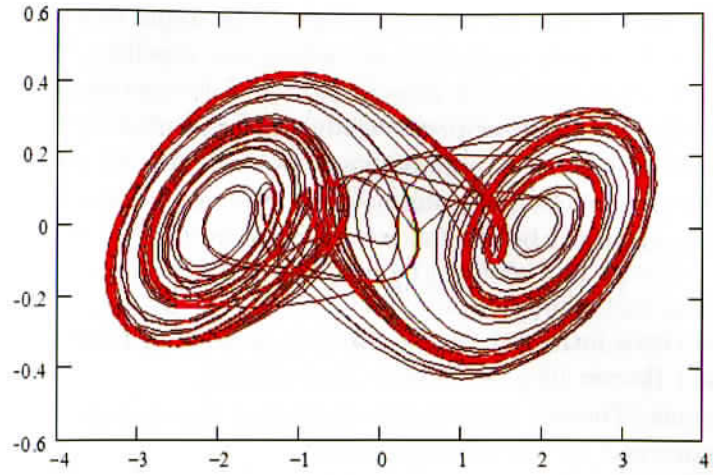

Fig. 4.7 Chaotic "double scroll" attractor ($a = 0.1, b = 0.1, \alpha = 15, \beta = 23$).

occurrence of a more complex type of the chaotic attractor, and is called a "doubled scroll" attractor. Its projection is shown in Fig. 4.7.

Chua circuit presents not only typical properties, being similar to the generator with MGIN model and to the Rössler model, but also exhibits a series of specific properties due to the symmetry. In the reference [Awrejcewicz and Calvisi (2002)] the proposals to build mechanical models/prototypes of the Chua circuit are given. A gallery of Chua's type attractors has been reported in the book by Bilotta and Pantano [Bilotta and Pantano (2008)], where nearly about 900 strange attractors have been detected, illustrated and discussed. The original Chua's system (4.17) containing five parameters $\alpha, \beta, \gamma, a, b$ can be further simplified to get a system with only one parameter of the form

$$\dot{x} = ay - x + (x+1) - (x-1), \qquad \dot{y} = z - x, \qquad \dot{z} = y. \tag{4.19}$$

The system (4.19) possesses a strange chaotic attractor for $a = 0.5$ ($\lambda_{\max} = 0.11$).

4.2.5 *Conservative and other systems*

The autonomous conservative systems in the language of mechanics refer to the lack of damping and gyroscopic forces. Systems without

damping and friction are rather unlikely to be found in nature, since they are indifferent, i.e. neither attractors nor repellers. In this and the next section, we do not present figures of strange chaotic attractors. On the contrary, we present only the differential equations and the values of associated parameters responsible for the occurence of a chaotic dynamics. A 3D autonomous system with quadratic nonlinearities governed by the following first order ODEs

$$\dot{x} = y, \quad \dot{y} = yz - x, \quad \dot{z} = \alpha - y^2, \tag{4.20}$$

exhibits chaos for $\alpha = 1$ ($\lambda_{\max} = 0.014$), and it has been studied by Nosé and Hoover [Hoover (1995); Nosé (1991)].

Thomas [Thomas (1999)] has discovered the so-called labyrinth chaos governed by the following ODEs

$$\dot{x} = \sin y, \quad \dot{y} = \sin z, \quad \dot{z} = \sin x, \tag{4.21}$$

where the state space is partitioned into 3D cells, and a trajectory wanders between the cells via a pseudorandom way.

The word *jerk* defines the derivative of acceleration and it is denoted by $\dddot{\vec{r}}$, where $\vec{r}$ is the position of a particle of mass m. In England, the word *jolt* is used instead of the word *jerk*. It is recommended to control the jerk of public transportation vehicles to avoid discomfort to passengers (it should be less than 2 ms^{-3}) or to avoid damage to transported fragile objects, like eggs. In addition, in the aerospace industry a sensor measuring jerk is used, and it is named a *jerkometer*.

Since the equation

$$\dddot{\vec{r}} = f(\ddot{\vec{r}}, \dot{\vec{r}}, \vec{r}) \tag{4.22}$$

can be projected onto one of the introduced rectangular co-ordinates, i.e. x, y or z, it yields a third-order differential ODE which can exhibit chaotic dynamics. Though a general approach to transform any three first-order ODEs to one "jerk" equation can be found elsewhere, one may observe that both Lorenz [Eq. (4.23)] and Rössler [Eq. (4.24)] systems have their counter part jerk forms as follows

$$\dddot{x} + (1 - \sigma + b - \dot{x}/x)\ddot{x} + [b(1 + \sigma + x^2) - (1 + \sigma)\dot{x}/x]\dot{x} - b\sigma(r - 1 - x^2)x = 0, \tag{4.23}$$

$$\dddot{y} + (c - a)\ddot{y} + (1 - ac)\dot{y} + cy - b - (\dot{y} - ay)(\ddot{y} - a\dot{y} + y) = 0. \tag{4.24}$$

The simplest quadratic jerk equation yielding chaos has been proposed by Sprott [Sprott (1997)], and it has the following form

$$\dddot{x} = -a\ddot{x} + \dot{x}^2 - x. \tag{4.25}$$

For $a = 2.02$, it gives a chaotic trajectory $x(t)$, and its largest Lyapunov exponent $\lambda_{\max} = 0.05$. The simplest cubic case of the jerk equation has been presented by Malasoma [Malasoma (2000)], and it reads

$$\dddot{x} = -a\ddot{x} + x\dot{x}^2 - x, \tag{4.26}$$

which exhibits chaos for $a = 2.03$ ($\lambda_{\max} = 0.08$). Another jerk equation studied by Malasoma [Malasoma (2002)] has the following form

$$\dddot{x} = -\alpha(x + \ddot{x}) + x\dot{x} + \dot{x}\ddot{x}/x, \tag{4.27}$$

which has been yielded by the systems

$$\dot{x} = z, \quad \dot{y} = -\alpha y + z, \quad \dot{z} = -x + xy. \tag{4.28}$$

The system governed by (4.27) exhibits chaos for $10.28 < \alpha < 10.37$, and its Kaplan–Yorke dimension $D_{ky} = 2.003$. Linz and Sprott [Linz and Sprott (1999)] presented the chaotic attractor of the jerk equation

$$\dddot{x} = -a\ddot{x} - \dot{x} + |x| - 1, \tag{4.29}$$

with an absolute value nonlinearity. For $a = 0.6$, the estimated $\lambda_{\max} = 0.036$. The already illustrated Lorenz attractor (Fig. 4.7) is known as a *two-scroll* attractor. The *three-scroll* system governed by equations

$$\dot{x} = x - yz, \quad \dot{y} = -y + xz, \quad \dot{z} = -3z + xy, \tag{4.30}$$

possesses also a chaotic attractor of $\lambda_{\max} = 0.378$. Finally, a four-scroll attractor can be exhibited by the following ODEs

$$\dot{x} = x - yz, \quad \dot{y} = x - y + xz, \quad \dot{z} = -3z + xy, \tag{4.31}$$

where the estimated largest $\lambda_{\max} = 0.248$.

The last example of three autonomous first-order ODEs exhibiting chaos deals with the so-called Rikitake dynamics [Rikitake (1958)]. The ODEs are as follows

$$\dot{x} = -\mu x + yz, \quad \dot{y} = -\mu y + x(z - \alpha), \quad \dot{z} = 1 - xy, \tag{4.32}$$

where the parameter α is responsible for the difference in the angular velocities of two disks, and the parameter α displays resistive dissipation. For $\alpha = \mu = 1$, Eq. (4.32) exhibits the two-scroll attractor with $\lambda_{\max} = 0.13$.

4.3 Non-Autonomous Systems

This section is devoted to simple nonlinear non-autonomous systems, which in the language of mechanics are simple stationary or non-stationary (parametric) oscillators usually harmonically excited.

We begin with the van der Pol externally excited oscillator governed by the second-order non-homogeneous differential equation of the form

$$\ddot{x} + b(x^2 - 1)\dot{x} + x = F \sin \omega t. \tag{4.33}$$

This equation has been studied by Cartwright and Littlewood [Cartwright and Littlewood (1945)], Levinson [Levinson (1949)], and more recently by Levi [Levi (1981)]. Strange attractor yielded by Eq. (4.33) can be obtained for $b = 1$, $F = 1$, $\omega = 0.45$, and the largest Lyapunov exponent $\lambda_{\max} = 0.04$.

Another equivalent example of a strange chaotic attractor is exhibited by the Rayleigh equation

$$\ddot{x} + (\dot{x}^2 - b)\dot{x} + x = F \sin \omega t \tag{4.34}$$

for fixed $b = 4$, $F = 5$, $\omega = 4$ ($\lambda_{\max} = 0.15$).

One of the simplest second-order non-autonomous ODEs is that of the following form

$$\ddot{x} + x\dot{x}^2 = \sin \omega t, \tag{4.35}$$

which exhibits chaos for $\omega = 4$ ($\lambda_{\max} = 0.014$). Certainly, the non-autonomous Duffing equation [Duffing (1918)] belongs to the

mostly revisited equations in mechanics, since numerous mechanical/physical systems can be modelled by it. It has the following form

$$\ddot{x} + c\dot{x} + \alpha_1 x + \alpha_2 x^3 = F \sin \omega t, \tag{4.36}$$

where chaos has been detected by Ueda [Ueda (1979)] and Moon and Holmes [Moon and Holmes (1979)]. In the mechanical language, the case $\alpha_1 > 0, \alpha_2 > 0$ corresponds to the stiffening elasticity of the system, whereas the case of $\alpha_1 > 0, \alpha_2 < 0$ describes the softening elasticity of the system. The latter one is also named as the Duffing two-well oscillator. The two-well oscillator with damping governed by the ODE

$$\ddot{x} + \dot{x} - x + x^3 = \sin \omega t, \tag{4.37}$$

displays a strange attractor for $\omega = 0.8$ with $\lambda_{\max} = 0.12$. Another example governed by equation

$$\ddot{x} + x^3 = \sin 2t \tag{4.38}$$

concerns a single-well oscillator exhibiting strange chaotic attractor with $\lambda_{\max} = 0.09$ [Gottlieb and Sprott (2001)].

Instead of a geometric-type nonlinearity one may take into account a piecewiselinear system of the form

$$\ddot{x} + |\dot{x} - x| + x - 2 = \sin t, \tag{4.39}$$

which possesses a strange chaotic attractor with $\lambda_{\max} = 0.08$. Two other examples deal with the so-called conservative signum oscillator

$$\ddot{x} + \operatorname{sgn} x = \sin t \tag{4.40}$$

and the exponential oscillator

$$\ddot{x} + \dot{x} + e^x - 1 = 21 \sin t, \tag{4.41}$$

where both of them have chaotic response. There also exists a documented research devoted to the analysis of simple oscillators parametrically and externally excited, governed by the following non-dimensional differential equation

$$\ddot{x} + \alpha\dot{x} + \omega_0^2(1 + h\cos(\nu t))x + \beta x^2 + \xi x^3 = \gamma \cos \omega t, \tag{4.42}$$

and this case has been extensively studied both analytically and numerically by Belhaq and Houssni [Belhaq and Houssni (1999)],

assuming that the difference between frequencies $\omega - \omega_0$ is small. In particular, it has been shown how the original quasi-periodic system, i.e. the parametric and external excitations having incommensurable frequencies, can be reduced to a periodically driven system. Chaotic behavior of this oscillator has already been reported in reference [Nayfeh (1983)] for $\xi = 0$.

The approximate analytical criteria of chaos occurrence have been proposed by Szemplińska–Stupnicka for $\xi = 0$ [Szemplińska–Stupnicka *et al.* (1989)]. Luo [Luo (2004)] gave analytical predictions of resonant separatrix bands and studied chaotic oscillations of the Mathieu–Duffing oscillator with a twin-well potential. Shen *et al.* [Shen *et al.* (2008)] investigated analytically the bifurcation route to chaos also in the Mathieu–Duffing oscillator. Luo and Yu [Luo and Yu (2014)] studied the case of Eq. (4.42) for $\xi = 0, \gamma = 0$. A route from periodicity to chaos has been illustrated and discussed via harmonic amplitudes varying with excitation amplitude in the finite term Fourier series solution. The case of equation (4.42) for $h < 0, \beta = 0$ for negative and positive spring constants putting emphasis to MEMS applications has been revisited in reference [Jin *et al.* (2014)]. Both Melnikov and Galerkin methods as well as the computation of the maximum Lyapunov exponents have been used to unveil the controllability of chaotic vibrations of the system driven by parametric pumps.

The Melnikov analytical and numerical techniques have been applied to study chaotic motions of the Duffing–Van der Pol oscillator with external and parametric excitations governed by the following equation

$$\ddot{x} + p\dot{x}(1 - x^2) - \alpha x + \beta x^3 = f(1 + \delta x)\cos \omega t, \tag{4.43}$$

in reference [Zhou and Chen (2014)]. The prediction of chaotic dynamics based on the Melnikov approach has been verified numerically.